Histology and
Histopathology
From Cell Biology to Tissue Engineering

ORIGINAL ARTICLE   **Open Access**

Maternal exposure to the environmental pollutant "BDE-47" impairs the postnatal development of rat cerebellar cortex by modulating neuronal proliferation, synaptogenesis, NGF and BDNF pathways

Dalia A. Mandour, Asmaa M. Tolba and Emtethal M. El-Bestawy

Department of Human Anatomy and Embryology, Faculty of Medicine, Zagazig University, Egypt

Summary. 2,2',4,4'-Tetrabromodiphenyl ether (BDE-47) is an environmental contaminant that crosses the blood placental barrier and interferes with the homeostasis of fetal thyroid hormones.

Aim of work. This study was designed to investigate the perinatal effect of BDE-47 exposure on the postnatal development of the rat cerebellar cortex.

Materials and methods. This study was carried out on 20 pregnant rats and 36 of their offspring. The pregnant rats were divided equally into control and BDE-47 treated mother groups; supplemented orally with BDE-47 (0.2 mg/kg/day from day 8 of gestation until the day of weaning). The offspring of both mother groups were subdivided, according to their developmental age, into three subgroups; PND14, PND21and PND42. SerumT3, T4 and TSH were assessed for dams and their offspring. Testing the motor coordination of the offspring via the rotarod test was conducted. Sections of the cerebellar cortex from offspring subgroups were stained with hematoxylin and eosin alongside immunohistochemical reactions and optical density of nerve growth factor (NGF), brain derived neurotrophic factor (BDNF), proliferating cell nuclear antigen (PCNA) and synaptophysin (SYN) were assessed. Also, the thickness of different layers of the cerebellar cortex was histomorphometrically measured.

Results. BDE-47 treated mothers and their offspring subgroups showed a significant decrease in the serum free T3, T4 and increased TSH. The BDE-47 offspring displayed incoordination of the motor activity together with disturbed cytoarchitecture of the cerebellar cortical layers, and impaired migration of its germinative neuronal zones, particularly on PND14 and PND21.

Moreover, these offspring displayed a decrease of the immune-expression and optical density of NGF, BDNF in the cerebellar cortical layers with impaired proliferation, and synaptogenesis.

Conclusion. Maternal exposure to BDE-47 during pregnancy and lactation effectuated a potential deleterious retarding effect on the postnatal development of the rat cerebellar cortex mostly via modulating neuronal proliferation, synaptogenesis, NGF and BDNF pathways secondary to its hypothyroid effect.

Key words: BDE-47, Cerebellar cortex, Development, Thyroid hormones, NGF, BDNF, PCNA, Synaptophysin, Rat offspring

Introduction

The cerebellum "little brain" is a well-characterized laminar structure that is situated at the midbrain-hindbrain junction. It is functionally concerned with

Corresponding Author: Asmaa Mohammed Tolba, Human Anatomy and Embryology Department, Faculty of Medicine, Zagazig University, Al-Kornish Street, Zagazig 44519, Egypt. e-mail: asmaaabdalaal1980@gmail.com or amtolba@zu.edu.eg

Abbreviations. ABC, Avidin-Biotin Complex; BDE-47, 2,2',4,4'-Tetrabrominated Diphenyl Ethers; BDNF, Brain Derived Neurotrophic Factor; BG, Bergmann glia cells; BW, Body Weight; Ca^{2+}, Calcium; DAB, 3,3'-Diaminobenzidine-tetrahydrochloride; EGL, External Granular Layer; GCL, Granular Cell Layer; GD, Gestational Day; H&E, Hematoxylin and Eosin; IGL, Internal Granular Layer; IHC, Immunohistochemical; LD, Lactational Day; ML, Molecular Layer; NGF, Nerve Growth Factor; NT-3, Neurotrophin-3; NT-4/5, Neurotrophin-4; 6-OH-BDE-47, 6 Hydroxylated 2,2',4,4'-Tetrabrominated Diphenyl Ethers; PBDEs, Polybrominated Diphenyl Ethers; PBS, Phosphate-Buffered Saline; PC, Purkinje cells; PCL, Purkinje cell layer; PCNA, Proliferating Cell Nuclear Antigen; PND, Postnatal Day; RIA, Radioimmunoassay; r.p.m, rotations per minute; sec, Seconds; SYN, Synaptophysin; T4, 3,5,3',5'-Tetraiodo-l-thyronine; T3, 3,5,3'-Triiodo-l-thyronine; THs, Thyroid Hormones; URL, Upper rhombic lip; ZSMRC, Zagazig Scientific Medical Research Center; ZU-IACUC, Zagazig University Institutional Animal Care and Use Committee.

coordination of the motor functions and postural adjustment (Roostaei et al., 2014). The cerebellum of most mammals is immature at birth and its histogenesis is usually accomplished within weeks of the postnatal period (Sánchez-Villagra and Sultan, 2002). Actually, the cerebellar growth and development is vulnerable and seriously affected by maternal exposure to some exogenous environmental factors, particularly during early embryogenesis and organogenesis which lead to disease susceptibility and acquisition in the offspring later in adulthood (Koning et al., 2017). Exogenous compounds like toxic agents, hypoxia, inflammation, infection, vitamin imbalance or hormonal status have adverse impacts on cerebellar development (Fonnum and Lock, 2000; Rees et al., 2008; Shevelkin et al., 2014).

Of particular interest, maternal exposure to a family of widely used flame retardant chemicals called polybrominated diphenyl ethers (PBDEs) were also documented to induce developmental toxicity of the offspring (Costa and Giordano, 2007). This is because these PBDEs can readily cross the blood-placental barrier and also accumulate in breast milk providing an opportunity for insulting the postnatal developmental processes (Kodavanti et al., 2015).

PBDEs are used in various household products such as plastics, furniture, electrical equipment, electronic devices, paints, construction materials, upholstery and textiles. Owing to their flame retardant properties, PBDEs release, at high temperatures, their bromine radicals that reduce the rate of combustion and dispersion of fire (Hooper and McDonald, 2000). Unfortunately, PBDEs form very weak covalent bonds to the polymers in those household products, so they readily leak into the surrounding environment delineating ubiquitous pollutants (Hites, 2004; Vuong et al., 2018). Subsequently, humans and animals are exposed to PBDEs through the inhalation of contaminated air, ingestion of contaminated food and via dermal absorption; in turn they bioaccumulate in different tissues of the body with diverse detrimental impacts on these tissues (Ni et al., 2012).

Recently, the adverse effects of PBDEs, as environmental pollutants, on the nervous system have received considerable attention. Exposure to PBDEs was linked with a cognitive dysfunction in humans (Lam et al., 2017) and was correlated with deficits of the memory in rodents (Dorman et al., 2018). The mechanisms for these neurotoxic effects were not fully elucidated, however, Kodavanti et al. (2015) have shown that PBDEs disturbed the thyroid hormones, caused oxidative stress, disrupted Ca^{2+}-mediated signal transduction and down-regulated the gene expression of some neurotrophic factors that collectively affect the development of the nervous system.

In this study, we have focused on the impact of 2,2',4,4'- tetrabromodiphenyl ether (BDE-47) which is one of the most stable, prevalent and biologically active among all known 209 PBDEs congeners. BDE-47 was reported to be massively accumulated in the surrounding environment and detected in blood, urine samples and breast milk of humans and animals with a correspondingly high tissue burden (Huang et al., 2010; Wu et al., 2015). In mammals, cytochrome p450 enzymes metabolize BDE-47 to a hydroxylated compound known as 6-OH-BDE-47 which is a potentially endocrine-disrupting molecule and has a more potential toxicity than the parent compound (Dingemans et al., 2008).

Previous studies have revealed that BDE-47 exposure was associated with liver toxicity (Suvorov and Takser, 2010), neurobehavioral toxicity (Koenig et al., 2012), thyroid toxicity (Talsness et al., 2008), and reproductive toxicity (Huang et al., 2015). However, to our knowledge, almost no available literature studies have highlighted postnatal cerebellar developmental toxicity following maternal exposure to BDE-47. Therefore, this current work was designed to evaluate the long-term impact of in utero and lactational exposure of this environmental pollutant, which is relevant to perinatal exposure experienced by humans, on the postnatal development of the rat cerebellar cortex.

Materials and methods

Chemicals

2,2',4,4'- tetrabromodiphenyl ether (BDE-47) powder, purity >99.5%, MW of 485.79 g/mol (Sigma-Aldrich, MO, USA). A fresh stock solution was freshly prepared daily, where 1mg of BDE-47 was dissolved in 10 ml of corn oil after sonication for 30 minutes at 40°C. Each pregnant rat was supplemented orally with 0.2 mg/kg BW (equivalent to 2ml/kg corn oil stock).

Experimental animals

Adult Sprague Dawley rats (twenty females and ten males) weighing180-220 g (9-12 weeks old) were used in this study. The rats were obtained from Zagazig Scientific Medical Research Center (ZSMRC) of Faculty of Medicine, Zagazig University. All rats were kept in polypropylene cages, maintained at 23±2°C, and a 12 h light/dark cycle with free access to a standard balanced chow diet and water ad libitum. Before the experiment, rats were acclimatized to the experimental conditions for one week. All rats were handled according to the standard guide for the care and use of laboratory animal research ethics issued and approved by Zagazig University Institutional Animal Care and Use Committee with reference number (ZU-IACUC/3/F/101/2021).

Female rat conception

Female and male rats, at a ratio of 2:1, were housed per a cage over night for mating. In the morning of the next day, vaginal smears were taken to assess the occurrence of pregnancy by detection of vaginal plug and sperm and that day was considered day zero of

gestation (GD0). Thereafter, each pregnant rat was kept alone in a cage till delivery, after which the dams and their pups were kept together, for lactation, until the time of weaning on PND21.The male pups only were selected for this study to cancel the cyclic hormonal fluctuation of females that represents a major confounder sex-different factor (González-Maciel et al., 2020), while the female pups were kept to be used in another protocol.

Experimental groups

Mother groups:

Twenty pregnant rats were divided randomly into two equal groups.

Control mother group (n=10):

Were supplemented orally with (2 ml/kg/day corn oil) as a vehicle from GD8 until the day of weaning on lactational day 21 (LD21).

BDE-47-treated mother group (n=10):

Were supplemented orally with (0.2 mg/kg/day of BDE-47) from GD8 until LD21 (Khalil et al., 2017).

Offspring Subgroups:

Eighteen pups of the control pregnant group and another eighteen pups of BDE-47 treated pregnant group were divided individually according to the day of postnatal sacrifice into 3 equal subgroups, of 6 pups each.
PND14 offspring subgroup.
PND21 offspring subgroup.
PND42 offspring subgroup.

Experimental procedure:

Blood samples from the retroorbital venous plexus of the mothers were taken on GD0, GD20 and LD21 and from the offspring subgroups at the time of their sacrifice on PND14, PND21 and PND42. The serum was separated and stored at -20°C for subsequent measurement of serum free T3, free T4, and thyroid stimulating hormone (TSH). Thereafter, all offspring subgroups were anesthetized using an intraperitoneal injection of sodium thiopental (40 mg/kg BW) then decapitated and the cerebellum was removed from the skull. Three cerebellar specimens were fixed in Bouin solution for 6 hours and three specimens were fixed in 10% neutral buffered formalin solution for 24 hours.

Rotarod test

The motor coordination of the rats was assessed using an accelerating rotarod apparatus (Ugo Basile, Varese, Model 7750, Italy). The test was performed according to the method described by Sałat et al. (2013) and Nagayach et al. (2014) with some minor modifications. Before the test, the rats were trained for three days; (3sessions/day, each session was 100 sec. with a starting speed of 2 rotations per minute (r.p.m) and a final maximum speed of 8 r.p.m). The test was conducted 24 hours after the final training trial. On the test day, the animals were placed in the direction that opposes the rotating rod and three sessions/day were performed; each session was started at 6 r.p.m and accelerated to final speed of 24 r.p.m. A resting time interval of 15 min. was allowed between each session. The time spent on the rotating rod before falling was recorded for each rat and the mean time was computed and recorded from the three sessions.

H&E staining

Bouin and formalin-fixed cerebellar specimens were dehydrated in ascending grades of ethanol, cleared in xylene, and embedded in paraffin blocks. Serial sagittal sections of 5 μm thick in the vermal region were cut and stained with H&E for routine histological examination of the cerebellar cortex of the offspring (Suvarna et al., 2018). The lobes and lobules of the cerebellar vermis were examined according to the consensus criteria established by Larsell and jonsen (1972). We obtained micrographs of the whole cerebellum (x40 magnification) by using the stitching procedure. In addition, images of x100 and x400 were obtained from the corresponding lobule of the central lobe of the vermal region in the age-matched groups of the control and BDE-47 offspring using a light microscope (Leica DM 500, Microsystems, AG, Heerbrugg, CH-9435, Switzerland) fitted with a digital camera (Leica ICC50 W camera) in the Anatomy Department, Faculty of Medicine, Zagazig University, Egypt).

Immunohistochemical (IHC) study

The paraffin blocks of the formalin-fixed specimens were utilized for IHC study. Paraffin sections of 4 μm thickness were mounted on positively charged slides, deparaffinized, hydrated and incubated with hydrogen peroxide to block endogenous peroxidase activity. Antigen retrieval and blocking of non-specific antigens were executed. Then, the slides were incubated with solutions of primary antibodies; Rabbit monoclonal anti-NGF (1:200, ab52918, Abcam, USA), anti-BDNF antibodies(1:200, ab213323, Abcam, USA), rabbit monoclonal anti-PCNA antibody (1:400, ab92552, Abcam, USA) and rabbit polyclonal anti-SYN antibody (1:400, PA527286, Thermo Scientific, USA). The slides with the primary antibodies were incubated with their corresponding biotinylated secondary antibodies and then conjugated with streptavidin horseradish peroxidase. Afterwards, a diaminobenzidine (DAB, Sigma-Aldrich Chemical Co., St. Louis, USA) chromogen solution was added to the slides to visualize the antigen–antibody-peroxidase reaction. Finally, the

sections were counterstained with Mayer's hematoxylin. Chromogen reaction yielded a brown-colored precipitate at the antigen sites (Ramos-Vara and Miller, 2014). Immunoreactivity was captured using Leica DM500, Microsystems, AG, Heerbrugg, CH-9435, Switzerland in the Anatomy Department, Faculty of Medicine, Zagazig University, Egypt.

Semi-quantitative histomorphometric assessment

Six non-overlapping H&E and immune-stained fields were selected from three different sections of the cerebellum of each subgroup of offspring on PND14, PND21, and PND42. H&E-stained sections were employed to estimate the thickness (μm) of the external granular layer (EGL), the molecular layer (ML), and the internal granular layer (IGL) at a magnification power x100, using the arbitrary distance method (three measurements were taken along the length of each layer/field). The immune-stained sections were used to evaluate the optical density of the immunohistochemical reaction to anti-NGF, anti-BDNF, anti-PCNA, and anti-SYN antibodies at magnification power x400 using ImageJ software analyzer computer system (Wayne Rasband, NIH, Bethesda, Maryland, USA). The mean values of these measurements were obtained and statistically analyzed.

Biochemical analysis

Serum levels of free T3, free T4, and TSH from the dams on GD0, GD20 and LD21 and from offspring subgroups at the time of sacrifice were measured by radioimmunoassay (RIA) according to the kit instructions (Siemens Healthcare Diagnostics, Germany). All samples were run in duplicate and the intra-assay coefficient of variation was 8.0%. The inter-assay variations ranged from 1% to 10%.

Statistical analysis

The histomorphometric and biochemical results were statistically analyzed using the statistical package of social science program (SPSS, version 19, Inc., Chicago, Illinois, USA). The quantitative data were expressed as Mean ± SD. Statistical comparison of the means of the two groups was performed using independent sample t-test. P value <0.05 was considered statistically significant.

Results

Behavior results

On assessing the motor coordination and the balancing time in sec. of the offspring using rotarod test, a very highly significant (p<0.001) decrease was found in the time spent by the BDE-47 offspring in relation to their age-matched control offspring (Table 1).

Results of H&E staining

H&E-stained sagittal sections of the cerebellar vermis of PND14 offspring subgroup of the control mothers showed the central lobe of the cerebellar cortex that lies in between the primary and secondary cerebellar fissures. The central lobe exhibited different lobules; declive, folium, tuber, and pyramid (Fig. 1a). Each lobule had four layers arranged from outside inwards; external granular layer (EGL), molecular layer (ML), Purkinje cell layer (PCL), and internal granular layer (IGL) with a white matter core having normal cellularity of this age group (Fig. 1c). The higher magnification of the folium lobule exhibited EGL (packed with small darkly stained granule cells), ML (having spindle-shaped migratory cells with small stellate and large basket cells), PCL (appeared as a single layer of Purkinje cells (PC) with Bergmann glial cell nuclei (BG) adjacent to their soma) and IGL (displayed small rounded deeply stained granule cells). The Purkinje cells appeared as large pear-shaped cells having large vesicular nuclei, prominent nucleoli and a rim of cytoplasm together with dendrites extending into ML (Fig. 1e).

H&E-stained sections of the cerebellar vermis of PND14 offspring of BDE-47 treated mothers revealed the central lobe of the cerebellar cortex to have the declive, folium, tuber, and pyramid. In these lobules, the EGL was thicker, while ML and IGL were thinner than the corresponding layers of the PND14 control offspring. Also, PC showed marked disarrangement. The white matter core of the lobules revealed marked cellularity (Fig. 1b,d). A higher magnification of the folium lobule showed a thicker EGL together with a thinner ML that revealed less migratory cells alongside scanty stellate and basket cells. The PCL displayed PC that were distributed in more than one layer and looked shrunken with numerous adjacent BG cells. The IGL exhibited compacted and aggregated small granule cells (Fig. 1f).

H&E-stained sagittal sections of the cerebellar vermis of PND21 control offspring showed the central lobe comprising the declive, folium, tuber, and pyramid. The lobules revealed more developmental differentiation, having a narrower EGL and less cellularity in the white matter core with sharp

Table 1. Influence of perinatal BDE-47 exposure on the motor coordination of the offspring subgroups at consecutive postnatal developmental periods PND14, PND21 and PND42.

Offspring	Control	BDE-47	P-value
Balancing time (sec.)			
PND14	32.16±6.17	15.66±3.61	<0.001
PND21	54.66±7.86	31.66±6.77	<0.001
PND42	67.50±7.81	42.83±6.30	<0.001

Data are expressed as mean±SD of 6 Offspring. Statistical comparison of the means values between two groups was performed using independent sample t-test. P value <0.001: very highly significant.

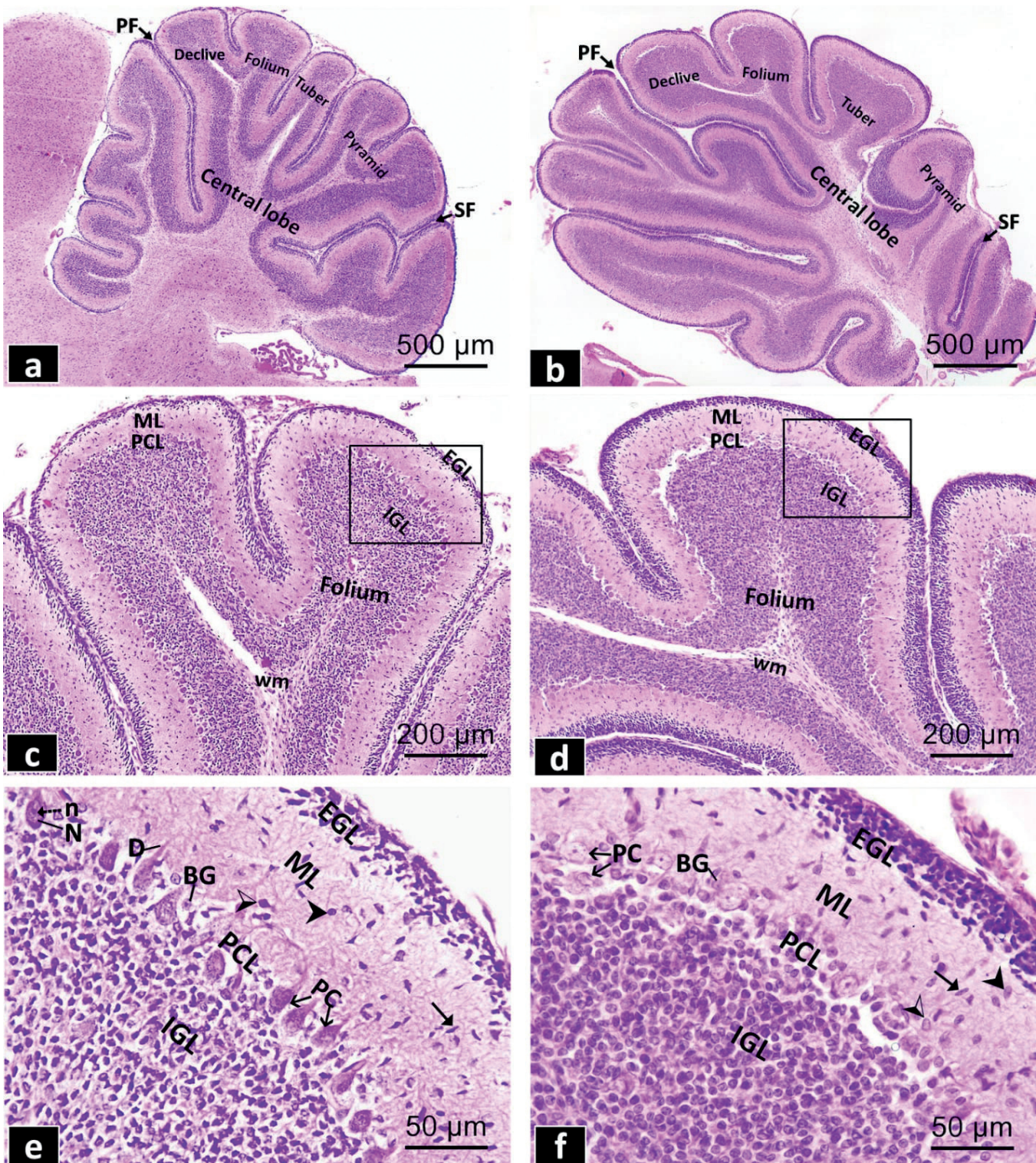**Fig. 1.** H&E-stained sagittal sections of the cerebellar vermis of PND14 offspring of the control and BDE-47 treated mothers. **a, b.** The control and BDE-47 offspring display the central lobe with its lobules; declive, folium, tuber, and pyramid between the primary (PF) and secondary (SF) fissures. **c, d.** The folium lobules of the control and BDE-47offspring reveal external granular layer (EGL), molecular layer (ML), Purkinje cell layer (PCL), and internal granular layer (IGL) with a white matter core (wm). However, there was a wider EGL and a marked cellularity of wm in BDE-47- offspring. **e.** A higher magnification of the squared area in the folium lobule of the control offspring exhibit EGL packed with darkly stained granule cells. ML shows stellate (black arrowhead), basket (semi-black arrowhead) and spindle-shaped migratory cells (black arrows). The PCL forms a single layer of large pear-shaped Purkinje cells (PC) having large vesicular nuclei (N), prominent nucleoli (n) and apical dendrites (D). Bergmann glial cell nuclei (BG) are multiple and adjacent to PC. The IGL exhibits predominantly small rounded deeply stained granule cells. **f.** A higher magnification of the squared area in the folium lobule of BDE-47offspring displays a thicker EGL with clumped small darkly stained granule cells and a thinner ML having less migratory cells (black arrow) alongside scanty stellate (black arrowhead) and basket (semi-black arrowhead) cells. The PCL exhibits disorganized shrunken PC that are distributed in more than one layer and numerous BG cells. IGL exhibits aggregated small granule cells.
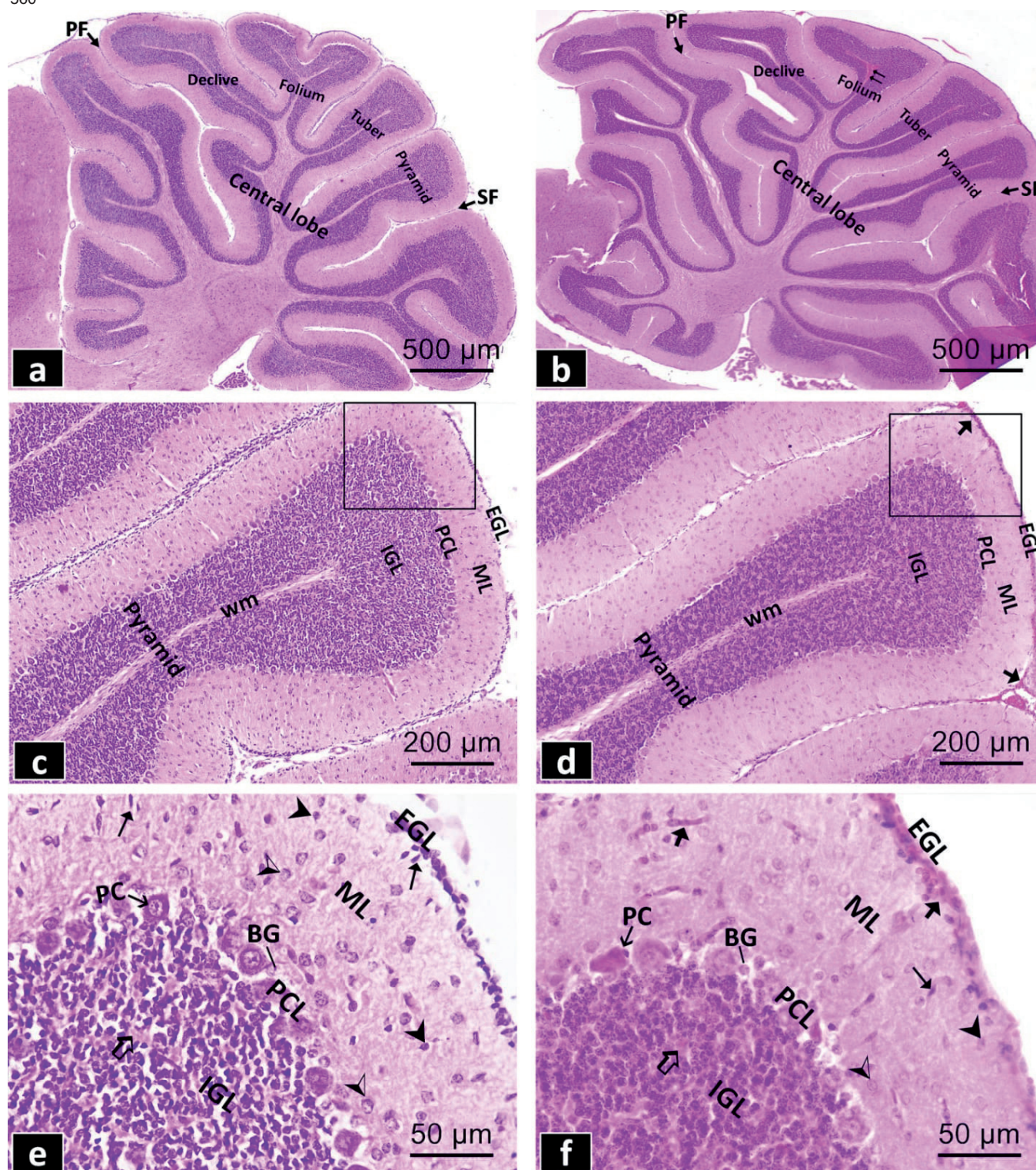
Fig. 2. H&E-stained sagittal sections of the cerebellar vermis of PND21 offspring of the control and BDE-47 treated mothers. **a, b.** The control and BDE-47 offspring display the central lobe with its lobules; declive, folium, tuber, and pyramid between the PF and SF. However, there are focal areas of hemorrhage (double arrow) in the white matter core of some cerebellar lobules in BDE-47-offspring. **c, d.** The pyramid lobules of the control and BDE-47 offspring showing EGL, ML, PCL, and IGL with a white matter core (wm). Moreover, EGL appears thicker with congested blood capillaries (black arrow), while ML seems thinner. **e.** A higher magnification of the squared area in the pyramid lobule of the control offspring demonstrates a remnant of EGL comprising a thin layer of darkly stained granule cells and the ML exhibits many migratory (black arrow), stellate (black arrowhead) and basket (semi-black arrowhead) cells. The PCL reveals a single layer of PC having large vesicular nuclei and BG cells. The IGL displays small deeply stained granule cells and well-developed glomeruli (white arrow). **f.** A higher magnification of the squared area in the pyramid lobule of BDE-47 offspring reveals thicker congested EGL with extravasated red blood cells (black arrow), the ML exhibits less migratory (small black arrow), stellate (black arrowhead), and basket (semi-black arrowhead) cells besides the congested blood capillaries (black arrow). The PCL contains shrunken PC having ill-defined pyknotic nuclei and deeply stained cytoplasm with loss of their apical dendrites. The BG cells appear multiple in between PC. The IGL exhibits aggregated granule cells with few glomeruli (white arrow).

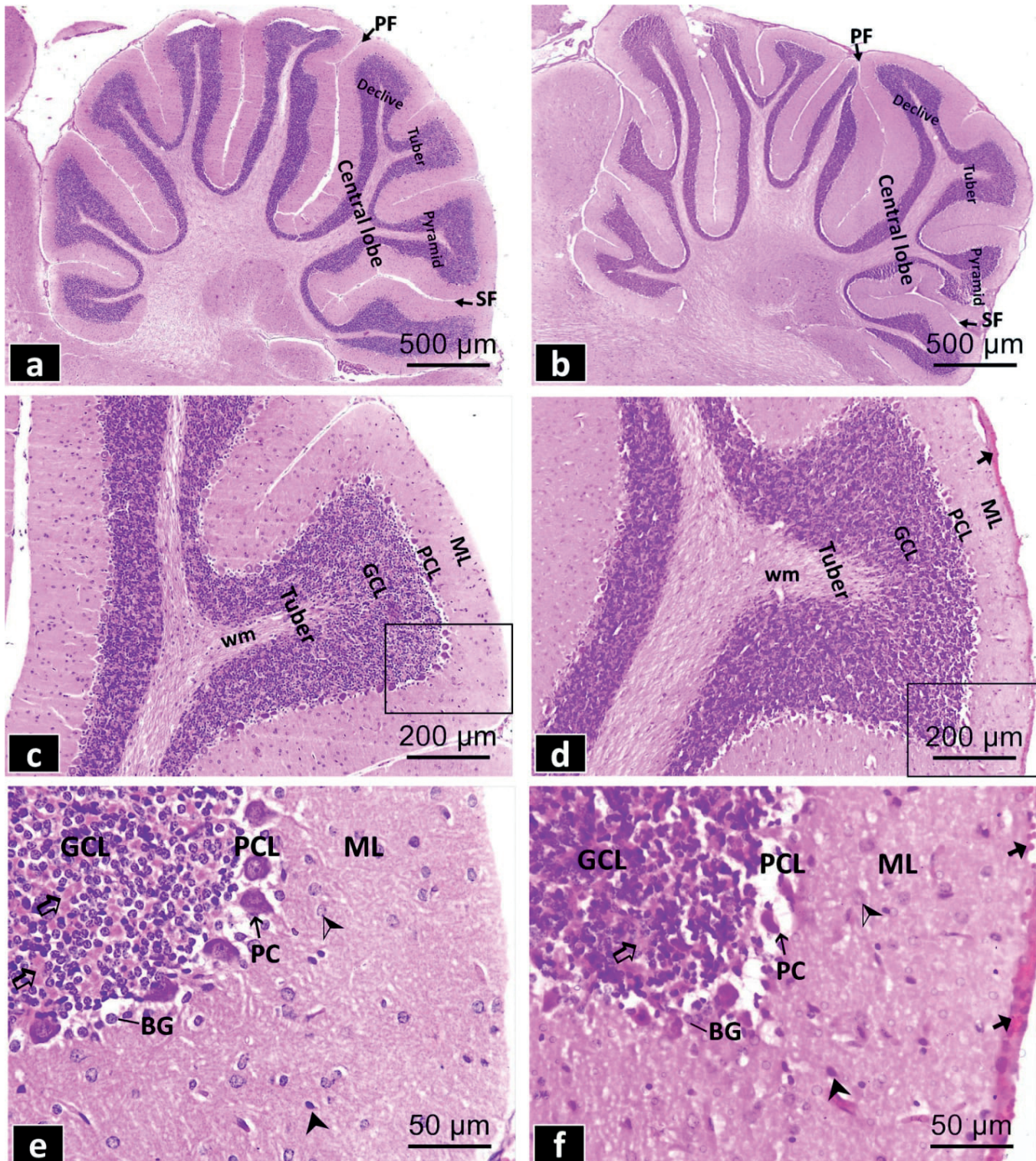*BDE-47" impairs the postnatal development of rat cerebellar cortex*

Fig. 3. H&E-stained sagittal sections of the cerebellar vermis of PND42 offspring of the control and BDE-47 treated mothers. **a, b.** The control and BDE-47 offspring display the central lobe between PF and SF. The BDE-47 offspring show apparent thinner lobules; declive, tuber, and pyramid. **c, d.** The tuber lobules of the control and BDE-47 offspring showing disappearance of EGL and white matter core (wm) is nearly devoid of cellularity. Moreover, BDE-47 offspring reveal extravasated red blood cells on the surface of the lobules (black arrow). **e.** A higher magnification of the squared area in the tuber lobule of PND42 control offspring exhibits ML with superficial stellate (black arrowhead), deep basket cells (semi-black arrowhead), and no migratory cells. The PCL shows PC with large nuclei with apical dendrites. BG cells are observed near the soma of PC. The GCL displays deeply stained granule cells and many glomeruli (white arrow). **f.** A higher magnification of the squared area in the tuber lobule of BDE-47 offspring reveals some stellate (black arrowhead) and basket (semi-black arrowhead) cells inside the neuropil of ML. The PCL displays BG cells adjacent to PC that exhibit shrunken cell bodies with pyknotic nuclei. The GCL exhibits clumped disorganized granule cells with some glomeruli (white arrow). Extravasated red blood cells are noticed on the surface of the lobules (black arrow).
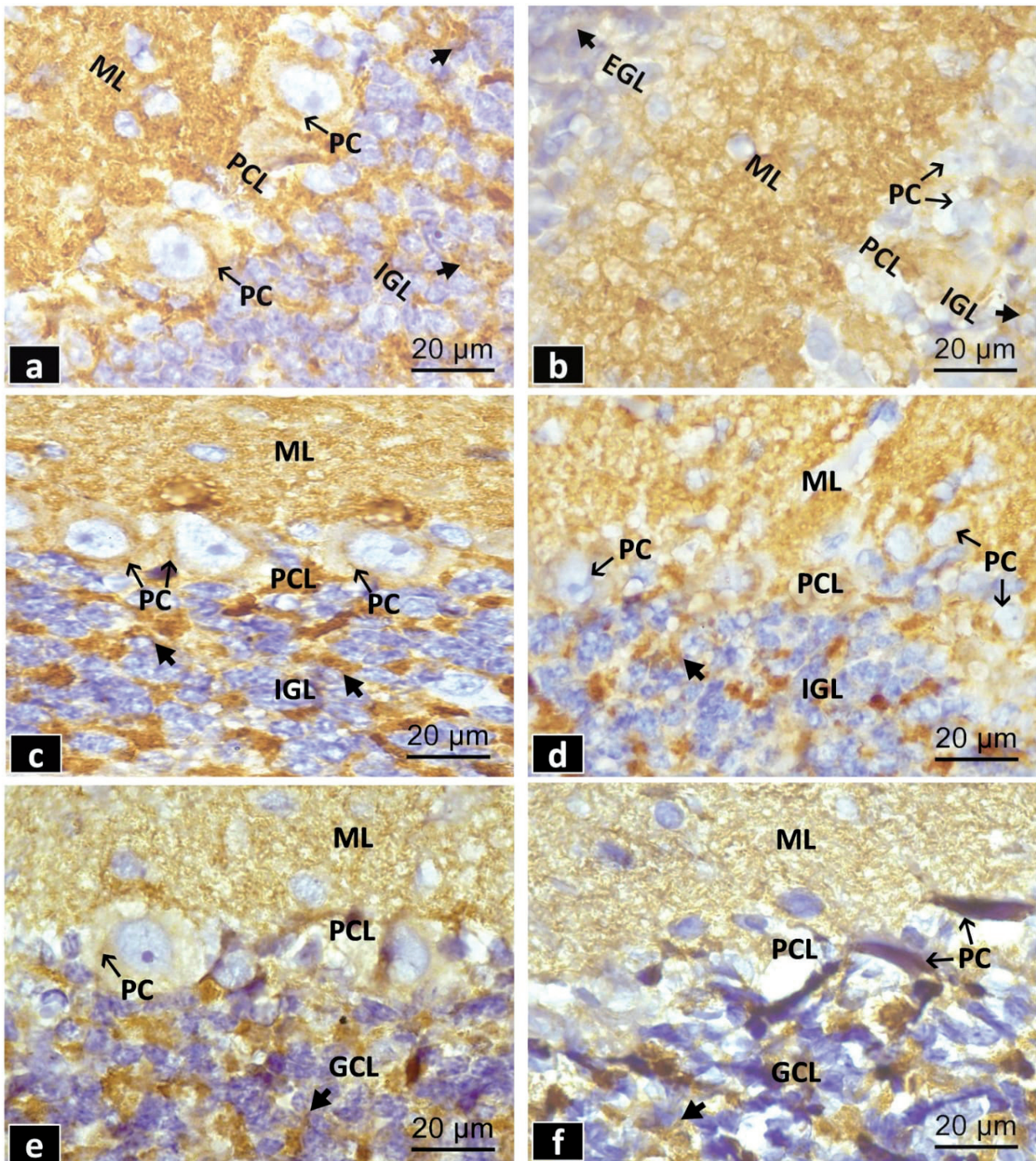
Fig. 4. NGF immuno-stained sagittal sections of the cerebellar vermis of PND14, PND21, and PND42 offspring of the control and BDE-47 treated mothers. **a, b.** The PND14 control offspring exhibit a strong NGF immunoreactivity in the granule cells (short arrow) of IGL and the neuropil of ML along with a moderate NGF expression in the cytoplasm (long arrow)of PC in PCL. On the other hand, the PND14 of BDE-47 offspring reveal a moderate NGF immunostaining in the granule cells (short arrow) of EGL, IGL, and in the neuropil of ML in addition to a weak expression in the cytoplasm (long arrow) of PC. **c, d.** The PND21 control offspring demonstrate a strong NGF immune expression in the granule cells of IGL and the neuropil of ML with a moderate expression in the cytoplasm (long arrow) of PC. On the contrary, the PND21 of BDE-47 offspring show a moderate NGF expression in the granule cells of IGL besides the neuropil of ML and a weak reactivity in PC. **e, f.** The PND42 control and BDE-47 offspring display a moderate NGF expression in ML and in the granule cells (short arrow) of the GCL and in the neuropil of ML. The cytoplasm (long arrow) of PC reveals a weak NGF expression in the control, but a negative expression in BDE-47 offspring. Immuno-peroxidase technique.
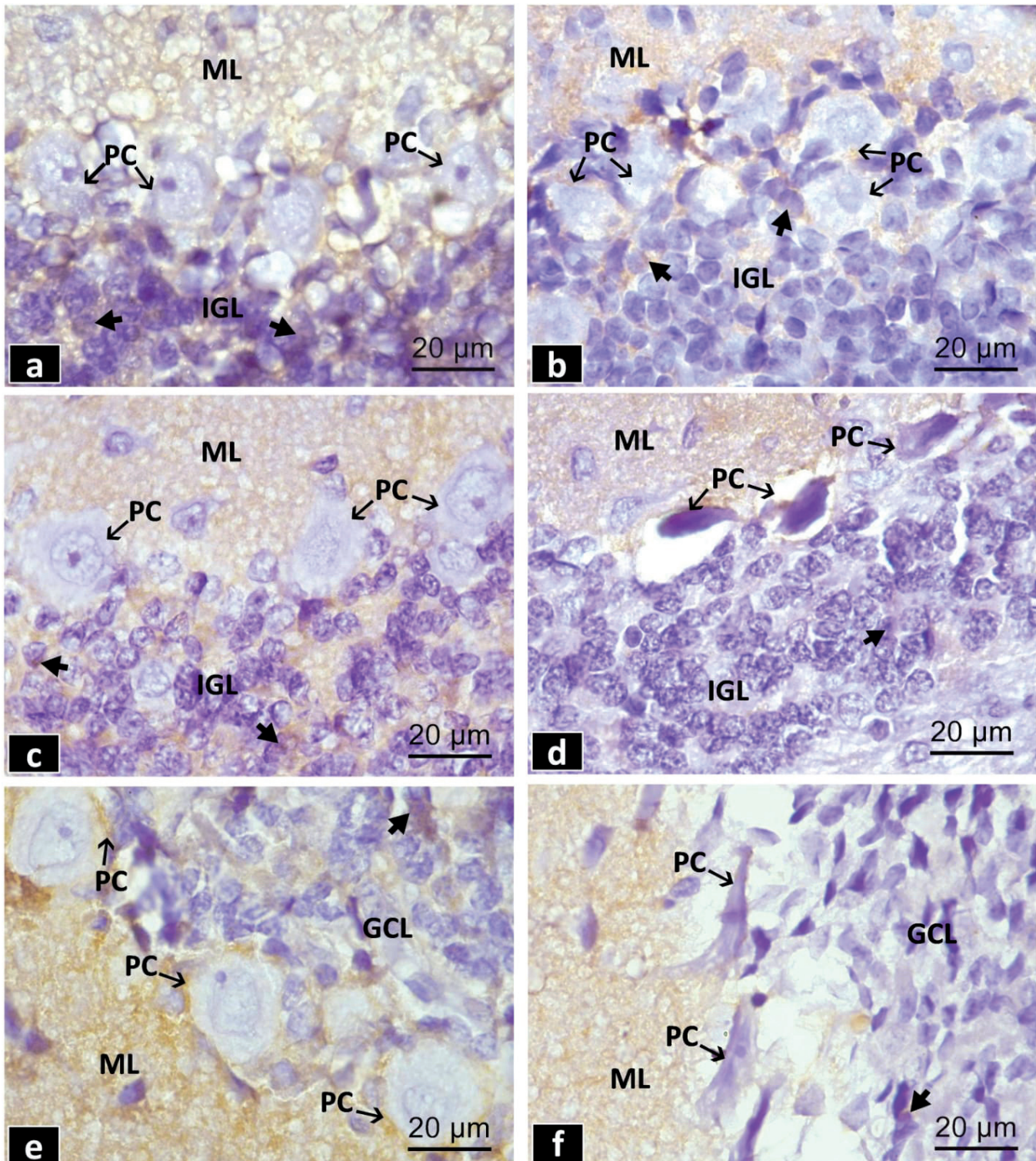
Fig. 5. BDNF immuno-stained sagittal sections of the cerebellar vermis of PND14, PND21, and PND42 offspring of the control and BDE-47 treated mothers. **a, b.** The PND14 control and BDE-47 offspring display a weak BDNF immune-expression in the granule cells (short arrow) of IGL and in the neuropil of ML. The cytoplasm (long arrow) of PC shows a weak BDNF expression in the control, with a negative expression in BDE-47 offspring. **c, d.** The PND21 control offspring show a moderate expression while BDE-47 offspring exhibit a weak BDNF expression in the granule cells (short arrow) of IGL and in the neuropil of ML. The cytoplasm (long arrow) of PC shows a weak BDNF expression in the control, with a negative expression in BDE-47 offspring. **e, f.** The PND42 control offspring display a strong BDNF expression in the granule cells (short arrow) of GCL and in the neuropil of ML while, the cytoplasm (long arrow) of PC shows a weak BDNF expression. On the other hand, the PND42 of BDE-47 offspring display a weak BDNF expression in the granule cells (short arrow) of GCL and in the neuropil of ML, while the cytoplasm (long arrow) of PC shows a negative expression. Immuno-peroxidase technique.
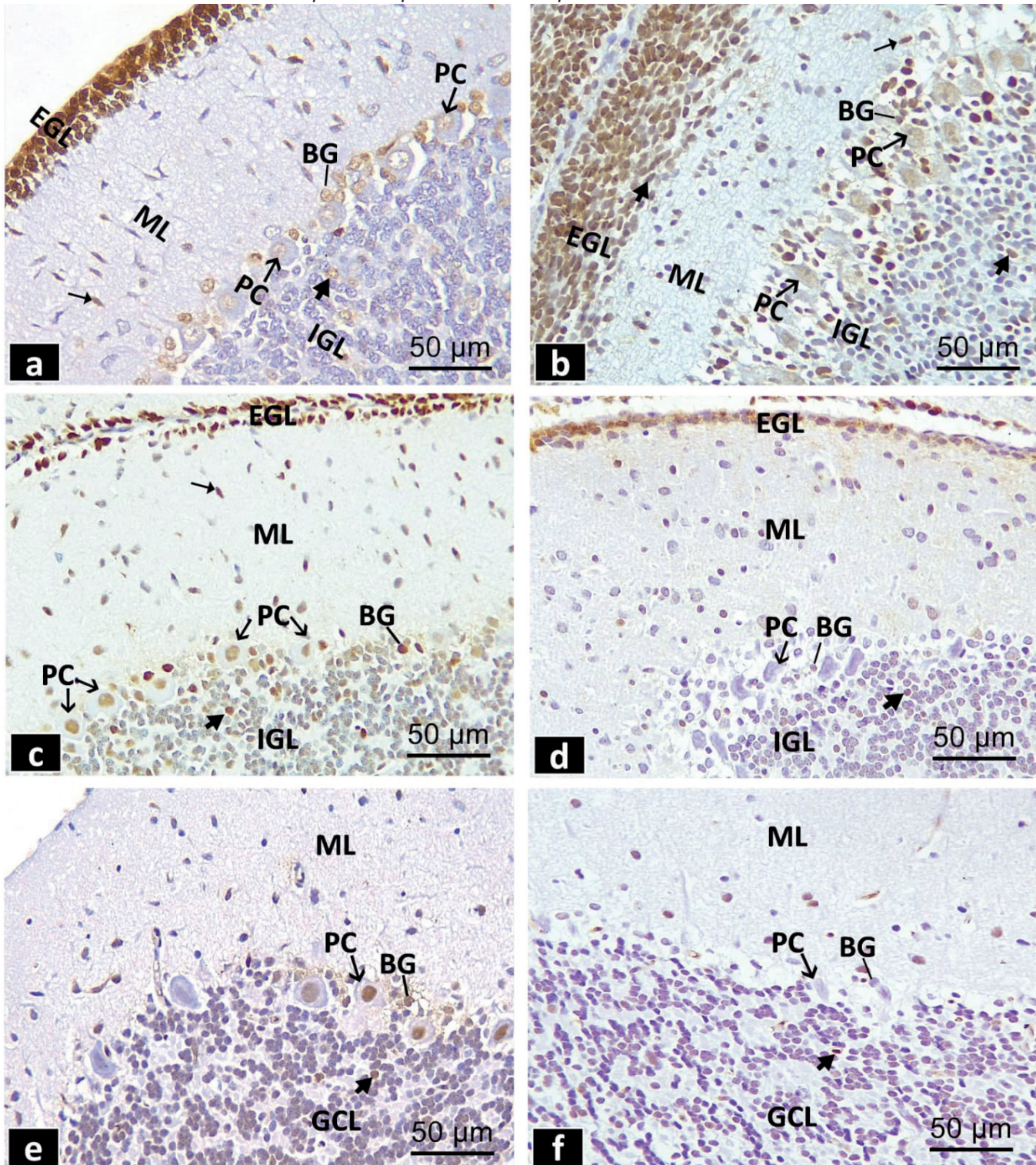
BDE-47" impairs the postnatal development of rat cerebellar cortex

Fig. 6. PCNA immuno-stained sagittal sections of the cerebellar vermis of PND14, PND21, and PND42 offspring of the control and BDE-47 treated mothers. **a, b.** The PND14 control offspring show a strong PCNA immune-expression, in EGL and the migratory cells (long arrow) in ML, along with a moderate expression in the nuclei of PC, BG cells, and the granule cells (short arrow) of IGL. On the other hand, the PND14 of BDE-47 offspring display a moderate PCNA immunostaining in the migratory cells (long arrow) and the granule cells (short arrow) of EGL and IGL. A strong PCNA immune-expression in BG cells, however PC display a weak PCNA immunoreaction. **c, d.** The PND21 control offspring show a strong PCNA immunoreactivity in EGL, and the migratory cells (long arrow) in ML, however they show a moderate expression in PC, BG cells, and the granule cells (short arrow) of IGL. On the contrary, the PND21 of BDE-47 offspring demonstrate a moderate PCNA immunoreaction in the granule cells (short arrow) of EGL, IGL, and in BG cells, alongside a negative immunoreaction in the PC. **e, f.** The PND42 control offspring demonstrating a weak PCNA in the nuclei of PC, BG cells, and the granule cells (short arrow) of GCL. By contrast, the PND42 of BDE-47 offspring reveal a weak PCNA expression in the granule cells (short arrow) of GCL, and in BG cells with a negative immunoreaction in PC. Immuno-peroxidase technique.
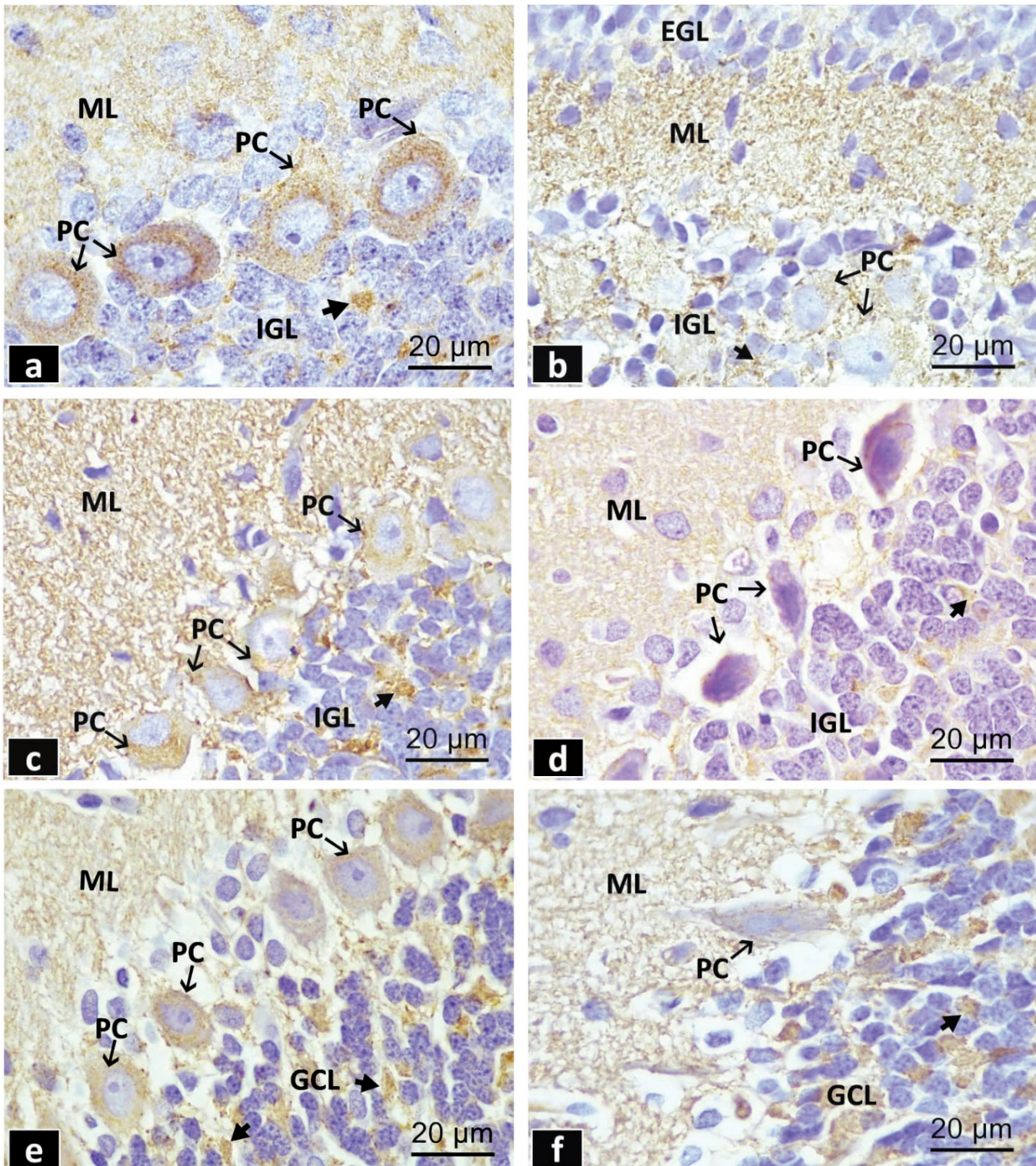
BDE-47" impairs the postnatal development of rat cerebellar cortex

Fig. 7. SYN immuno-stained sagittal sections of the cerebellar vermis of PND14, PND21, and PND42 offspring of the control and BDE-47 treated mothers. **a, b.** The PND14 control offspring show a strong SYN immune-expression that appears as brown beaded granules at the surface of the neuronal cell bodies of PC and in their cytoplasm (long arrow), in the neuropil of ML, and the glomeruli (short arrow) in IGL. On the other hand, the PND14 offspring of BDE-47 reveal a moderate SYN immunoreactivity in PC, the neuropil of ML, and faintly stained reactive granules in IGL with a negative SYN expression in EGL. **c, d.** The PND21 control offspring demonstrate a moderate SYN expression in PC (long arrow), the neuropil of ML and the glomeruli (short arrow) in IGL. On the contrary, the PND21 offspring of BDE-47 show a weak SYN immunostaining in PC, the neuropil of ML, and the glomeruli (short arrow) in IGL. **e, f.** The PND42 control offspring exhibit a moderate SYN expression in PC, the neuropil of ML, and the glomeruli (short arrow) in GCL. On the other hand, the PND42 offspring of BDE-47 display a weak SYN immunoreactivity in PC, the ML, and the glomeruli (short arrow) in GCL. Immuno-peroxidase technique.

demarcation from IGL compared with PND14 control offspring (Fig. 2a,c). A higher magnification of the pyramid lobule showed a remnant of EGL and the ML exhibited many spindle-shaped migratory, stellate, and basket cells. The PCL had a single layer of well-arranged PC with their characteristic large vesicular nuclei and long dendrites extending into ML together with BG cells adjacent to their soma. The IGL displayed small rounded deeply stained granule cells and well-developed glomeruli that appeared as acidophilic non-cellular areas (Fig. 2e).

H&E-stained sections of the cerebellar vermis of PND21 offspring of BDE-47-treated mothers revealed the central lobe having its characteristic four lobules that showed apparently thicker EGL, while ML and IGL appeared thinner than the corresponding layers of PND21 control offspring. The white matter core revealed focal areas of hemorrhage (Fig. 2b,d). A higher magnification of the pyramid lobule showed congested EGL with extravasated red blood cells, the ML exhibited less migratory, stellate, and basket cells alongside congested blood capillaries. The PCL contained shrunken PC having pyknotic nuclei, deeply stained cytoplasm, and loss of their apical dendrites. The BG cells appeared multiple in between PC. The IGL exhibited aggregated granule cells, with few glomeruli (Fig. 2f).

H&E-stained sagittal sections of the cerebellar vermis of PND42 control offspring showed the central lobe with its lobules. These lobules revealed a more cerebellar development involving disappearance of EGL, and hence the IGL was substituted with the granule cell layer (GCL) and well-developed white matter core with the cellular component was hardly seen compared to PND21 control offspring (Fig. 3a,c). A higher magnification of the tuber lobule showed a wide ML with well-developed stellate and basket cells with absent migratory cells. The PCL appeared as a single layer of PC having large nuclei and prominent nucleoli with adjacent BG cells. The GCL displayed deeply stained granule cells and multiple well-developed glomeruli

(Fig. 3e).

H&E-stained sections of the cerebellar vermis of PND42 offspring of BDE-47 treated mothers displayed the central lobe with the disappearance of EGL of its lobules. Congested blood capillaries and extravasated red blood cells were observed on the surface of the lobules (Fig. 3b,d). A higher magnification of the tuber lobule showed the ML having stellate and basket cells but no migratory cells. The PCL displayed BG cells adjacent to the PC that exhibited shrunken cell bodies with loss of their apical dendrites. The GCL had clumped disorganized granule cells with some glomeruli (Fig. 3f).

Results of NGF immunohistochemical staining

The PND14 and PND21 offspring of the control mothers revealed a strong NGF immune-expression in the cytoplasm of the granule cells of the EGL and IGL and in the neuropil of ML. The PCL exhibited a moderate NGF expression in the cytoplasm of PC (Fig. 4a,c). The PND42 control offspring revealed a moderate NGF expression in the ML and in the cytoplasm of the granule cells of GCL with a weak expression in the cytoplasm of the PC (Fig. 4e).

The PND14 and PND21 offspring of BDE-47 treated mothers showed a moderate NGF immune-expression in the cytoplasm of the granule cells of the EGL and IGL together with the neuropil of the ML, alongside a weak expression in the cytoplasm of PC (Fig. 4b,d). The PND42 offspring of BDE-47 treated mothers displayed a moderate NGF expression in the ML and in the cytoplasm of the granule cells of the GCL with a negative NGF immunoreactivity in the PC (Fig. 4f).

Results of BDNF immunohistochemical staining

The PND14 offspring subgroup of the control mothers revealed a weak BDNF immune-expression in the cytoplasm of the granule cells of both EGL and IGL,
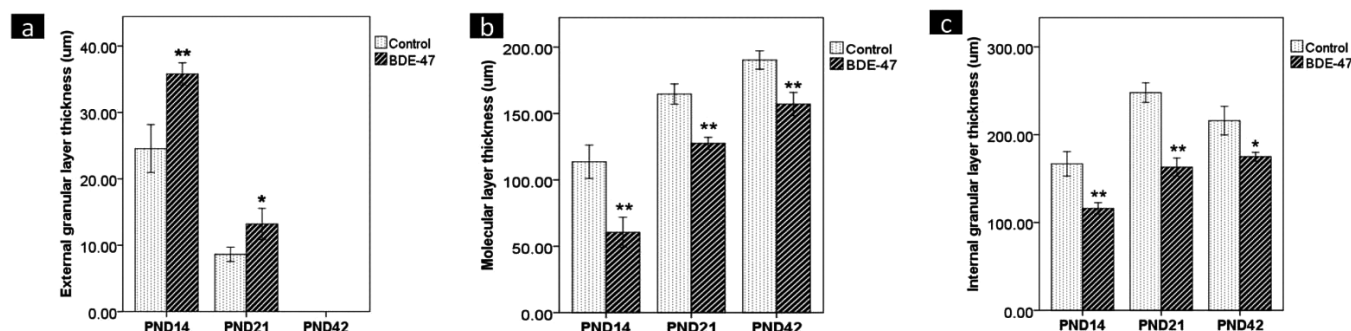
Fig. 8. Bar charts showing the effect of perinatal exposure to BDE-47 on the thickness of EGL **(a)**, ML **(b)**, and IGL **(c)** in the rat vermal cerebellar sections of the offspring subgroups at consecutive postnatal developmental periods PND14, PND21 and PND42. Statistical comparison of the mean values between two groups was done using independent sample t-test. *= highly signifiant (P<0.01),** = very highly significant (P<0.001).

in the neuropil of ML, and in the cytoplasm of PC (Fig. 5a). The PND21 control offspring exhibited a moderate BDNF expression in the granule cells of both EGL and IGL, and in the neuropil of ML, while a weak expression was noticed in the cytoplasm of PC (Fig. 5c). The PND42 control offspring revealed a strong BDNF immune-expression in the granule cells of GCL and the neuropil of ML, while a weak expression was noticed in the cytoplasm of PC (Fig. 5e).

The PND14, PND21, and PND42 offspring subgroups of the BDE-47treated mothers showed a weak BDNF expression in the granule cells of EGL and IGL (in the first two age subgroups), GCL (in the third subgroup) and in the neuropil of ML of all subgroups. A negative BDNF expression was observed in the cytoplasm of PC of all subgroups (Fig. 5b,d,f).

Results of PCNA immunohistochemical staining

The PND14 and PND21 offspring of the control mothers revealed a strong PCNA immune-expression in the EGL and the migratory cells in the ML, while the nuclei of PC and BG cells together with the granule cells of IGL displayed a moderate PCNA immunoreactivity (Fig. 6a,c). The PND42 control offspring displayed a weak PCNA immunoreactivity in the nuclei of PC, BG cells, and the granule cells of GCL (Fig. 6e).

The PND14 offspring of BDE-47 treated mothers showed a moderate PCNA immunostaining of the granule cells of the EGL and IGL, the migratory cells in ML, while the BG cells exhibited a strong PCNA immune-expression. The PC displayed a weak PCNA immunoreaction (Fig. 6b). The PND21 offspring of BDE-47 treated mothers exhibited a moderate PCNA immune-reaction in the granule cells of EGL, IGL, and BG cells alongside a negative immunoreaction in the PC (Fig. 6d). The PND42 offspring of BDE-47 treated mothers showed a weak PCNA immunoreaction in the granule cells of GCL, and BG cells with a negative immunoreaction in PC (Fig. 6f).

Results of SYN immunohistochemical staining

The PND14 control offspring revealed a strong SYN immunoreactivity at the surface and the cytoplasm of PC, in the neuropil of ML and the cerebellar glomeruli in IGL (Fig. 7a). The PND21 control offspring exhibited a moderate SYN expression in PC, the neuropil of ML, and the glomeruli in IGL (Fig. 7c). The PND42 control offspring exhibited a moderate SYN expression in PC, the neuropil of ML and the glomeruli in GCL (Fig. 7e).

The PND14 offspring of BDE-47 treated mothers showed a moderate SYN immunoreactivity at the surface and the cytoplasm of PC, in the neuropil of ML,
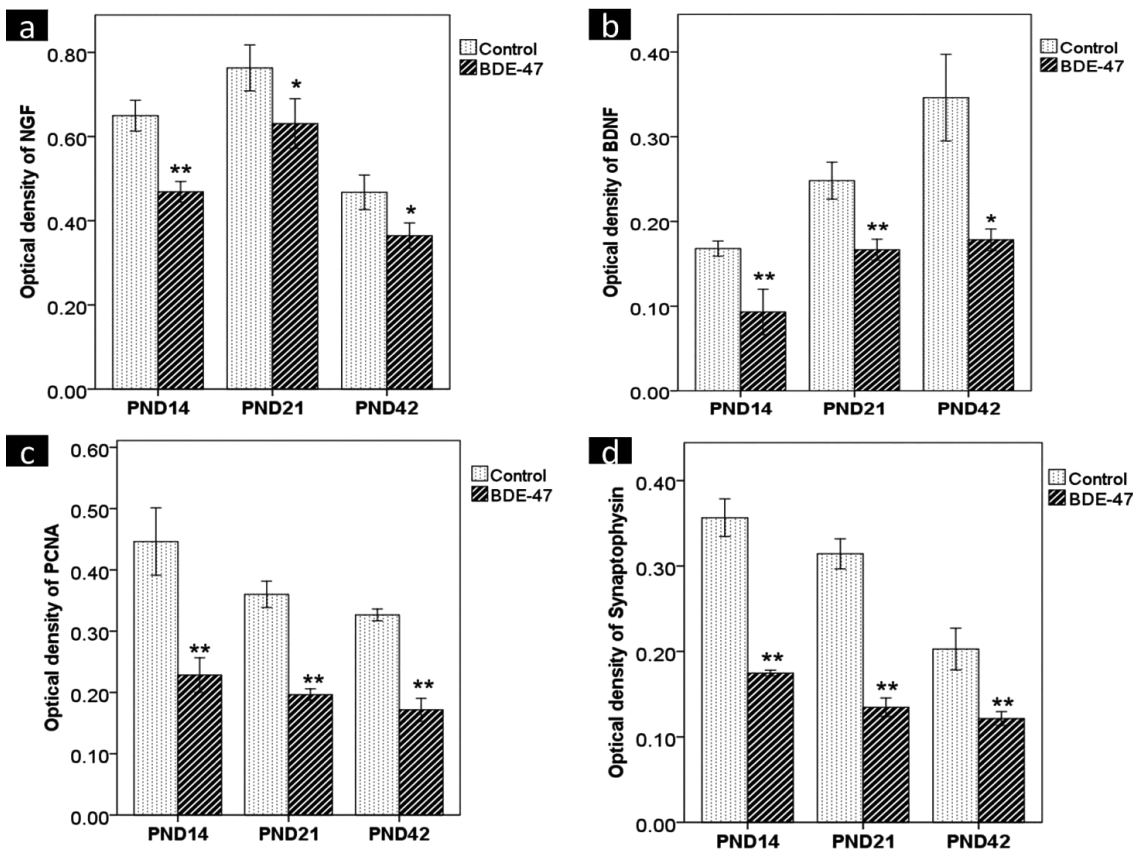

Fig. 9. Bar charts showing the effect of perinatal exposure to BDE-47 on the optical density of NGF **(a)**, BDNF **(b)**, PCNA **(c)**, and SYN **(d)** immunostaining in the rat vermal cerebellar sections of the offspring subgroups at consecutive postnatal developmental periods (PND14, PND21 and PND42). Statistical comparison of the mean values between two groups was done using independent sample t-test. *= highly signifiant (P<0.01),** = very highly significant (P<0.001).

and IGL along with a negative SYN immune-expression in EGL (Fig. 7b). The PND21 offspring of BDE-47 exhibited a weak SYN immunostaining in PC, the neuropil of ML, and the glomeruli in IGL (Fig. 7d). Also, the PND42 offspring of BDE-47 treated mothers displayed a weak SYN immunoreactivity in PC, the ML, and the glomeruli in GCL (Fig. 7f).

Histomorphometric results

The mean thickness of the external granular layer (EGL) of the cerebellar cortex in the vermis region of PND14 offspring subgroup of BDE-47-treated mothers showed a very highly significant increase (P<0.001) as compared to the corresponding age matched control subgroup, while on PND21 there was a highly significant increase (P<0.01) in the mean thickness of EGL in BDE-47 offspring in comparison to the corresponding layer of control offspring. EGL developmentally disappeared in both PND42 control and BDE-47 offspring (Fig. 8a).

A very highly significant decrease (P<0.001) in the mean thickness of the molecular layer (ML) was recorded in the PND14 and PND21 and PND42 of BDE-47 offspring in comparison to the age-matched control offspring (Fig. 8b).

A very highly significant decrease (P<0.001) in the mean thickness of the internal granular layer (IGL) was detected in the PND14 and PND21 of BDE-47 offspring compared to the age-matched control offspring, while on PND42 there was a highly significant decrease (P<0.01) in the mean thickness of IGL of BDE-47 offspring compared to the control offspring (Fig. 8c).

The mean optical density of NGF immunostaining of the vermal cerebellar sections in PND14 of BDE-47 offspring showed a very highly significant decrease (P<0.001) as compared to the control offspring, while in PND21 and PND42 of BDE-47 offspring, there was a highly significant decrease (P<0.01) in optical density of NGF immunostaining as compared to the corresponding control offspring (Fig. 9a).

The mean optical density of the cerebellar BDNF immunostaining in PND14 and PND21 of BDE-47 offspring showed a very highly significant decrease (P<0.001) as compared to the corresponding age matched control, while in PND42 of BDE-47 offspring there was a highly significant decrease (P<0.01) in BDNF optical density as compared to the corresponding control subgroup (Fig. 9b).

The mean optical density of the cerebellar PCNA immunostaining revealed a very highly significant decrease (P<0.001) in all BDE-47 offspring subgroups (PND14, PND21 and PND42) as compared to the corresponding control subgroups (Fig. 9c).

The statistical comparison of the mean value of the optical density of the cerebellar SYN immunostaining at different postnatal developmental periods revealed a very highly significant decrease (P<0.001) in all BDE-47 offspring subgroups (PND14 and PND 21 and PND42) as compared to the corresponding control subgroups (Fig. 9d).

Biochemical results

The mean serum levels of free T3, T4 and TSH in the control and BDE-47-treated dams at GD0 showed a non-significant difference (P>0.05). At GD20 and LD21, there was a very highly significant decrease (P<0.001) in T3 and T4. However, TSH mean serum levels of BDE-47 treated dams at GD20 showed a highly significant increase (P<0.01) as compared to the control dams,

Table 2. Influence of perinatal BDE-47 exposure on serum free T3, freeT4 and TSH of the dams at GD0, GD20, and LD21.

		Control	BDE-47	P-value
T3 (ng/ml)				
	GD0	0.82±0.10	0.80±0.09	>0.05
	GD20	2.64±0.60	0.58±0.09	<0.001
	LD21	0.93±0.12	0.21±0.24	<0.001
T4 (µg/dl)				
	GD0	2.67±0.41	2.5 ±0.43	>0.05
	GD20	3.70±0.41	1.29±0.26	<0.001
	LD21	2.88±0.45	0.55±0.11	<0.001
TSH (µIU/ml)				
	GD0	0.73±0.06	0.71±0.09	>0.05
	GD20	0.52±0.09	2.45±0.56	<0.01
	LD21	0.65±0.05	3.66±0.41	<0.001

Data are expressed as mean±SD of 10 dams. Statistical comparison of the mean values between two groups was performed using independent sample t-test. P value >0.05: insignificant, <0.01: highly significant, and <0.001:very highly significant. GD0:gestational day zero, GD 20: gestational day twenty, LD 21: lactational day 21.

Table 3. Influence of perinatal BDE-47exposure on the serum free T3, freeT4, and TSH of the offspring subgroups at consecutive postnatal developmental periods PND14, PND21 and PND42.

Offsring Subgroups	Control	BDE-47	P-value
T3 (ng/ml)			
PND14	0.25±0.05	0.12±0.01	<0.001
PND21	0.31±0.04	0.18±0.02	<0.001
PND42	0.50±0.33	0.34±0.04	<0.001
T4 (µg/dl)			
PND14	0.98±0.15	0.32±0.14	<0.001
PND21	1.26±0.05	0.51±0.05	<0.001
PND42	1.92±0.18	1.14±0.08	<0.001
TSH (µIU/ml)			
PND14	0.56±0.03	2.63±0.18	<0.001
PND21	0.40±0.04	1.22±0.14	<0.001
PND42	0.28±0.03	0.72±0.10	<0.05

Data are expressed as mean±SD of 6 Offspring. Statistical comparison of the mean values between two groups was performed using independent sample t-test.P value <0.05: significant and <0.001:very highly significant.T3:Triiodothyronine,T4:Tetraiodothyronine, and TSH: thyroid stimulating hormone.

while at LD21 a very highly significant increase (P<0.001) in TSH was recorded as compared to the control dams (Table 2).

Avery highly significant decrease (P<0.001) in serum T3 and T4 in all BDE-47 offspring was encountered as compared to the control offspring. Regarding serum TSH level, in BDE-47 offspring, there was a very highly significant increase (P<0.001) on PND14 and PND21, while a significant increase (P<0.05) was recorded on PND42 as compared to the control offspring (Table 3).

Discussion

In this study, in utero and lactational exposure to BDE-47 revealed remarkable histopathological changes in the cytoarchitecture of the cerebellar cortex of the offspring at the three studied postnatal developmental periods. Obviously, a thicker EGL was detected at the histological examination of PND14 and PND21 offspring of BDE-47 treated mothers compared to the age-matched control offspring. This finding suggested a delay in the normal migration of the granule cells from the EGL into the IGL passing through the ML. Moreover, more cellularity of the white matter core of the cerebellar lobules was observed under light microscope on PND14 and PND21 offspring of BDE-47 treated mothers and this indicated a longer persistence of the cellular hub of this white matter core that also pointed to a delayed migration of the precursor cells resident in this core to their target destination layers at IGL and ML.

The mechanism of the delayed migration of the aforementioned granule and precursor cells of the cerebellum of BDE-47 offspring could be attributed indirectly to the interference of this environmental pollutant with the synthesis of thyroid hormones that are essential for the normal neuronal migration and differentiation (Ahmed et al., 2012; Bansal et al., 2014). The hypothyroid effect of BDE-47 was evident in the present study upon measuring the serum thyroid hormones and TSH in the dams and their offspring subgroups. Being a brominated hydrocarbon compound, BDE-47 has a hypothyroid effect via impeding the thyroid hormones biosynthesis through its bromide constituents that competitively inhibit the active iodine uptake by the thyroid gland (Bansal et al., 2014). Importantly, the delay in migration of the cerebellar cortical cells upon perinatal exposure to BDE-47 reflected a delay in the postnatal development of the cerebellum. Actually, neuronal migration is a fundamental process that brings the developing cerebellar neurons to their final destination with an appropriate spatio-temporal pattern and provides an assembly of functioning neuronal circuits (Rahimi-Balaei et al., 2018).

Developmentally, in rats and mice, cerebellar neuronal migration starts in the immature mammalian cerebellum that has six different types of precursor interneurons (two excitatory glutamatergic and four inhibitory GABAergic interneurons). The excitatory interneurons include the granule and unipolar brush cells that originate from a primary germinal zone called the upper rhombic lip (URL) and migrate to a secondary germinative zone (the EGL). The unipolar brush cells migrate directly to the IGL by PND10, while the granule cells migrate through the ML and the PCL to reach their final position in the IGL around the PND20. The inhibitory interneurons include Golgi, Lugaro, stellate, and basket cells originating from another primary germinal zone called the cerebellar plate ventricular zone and migrate to the secondary germinative zone (the white matter core). Thereafter, Golgi cells migrate to IGL by PND4, Lugaro cells migrate to the top of the IGL by PND5, while basket and stellate cells migrate through the IGL and PCL to their final destination in the ML by PND16 (Galas et al., 2017).

In the context of the above-mentioned normal neuronal migration of the cerebellar precursor's interneurons, in this work, it was observed that in the control offspring the thickness of the EGL decreased sequentially from PND14 to be a rim on PND21 and also the stellate and the basket cells were numerously detected in the ML on PND21. This denoted that the granule, the stellate, and the basket have reached their final destination at that developmental age. These two great histological observations in this study might imply that the postnatal development of the cerebellar cortex was nearly accomplished on PND 21 in rats. This finding was aligned with the hypothesis of this study that the structural and functional maturation of the rat cerebellum occurs mainly postnatally and this is why we intentionally chose the three postnatal developmental periods (PND14, 21, and 42) (Djatchkova-Podkletnova and Alho, 2005).

In contrast to what was found in the control offspring, the BDE-47 offspring displayed a retarded postnatal development of the cerebellar cortex. This deleterious effect of BDE-47 could be attributed mainly to the hypothyroid impact of this compound. Our assumption was in line with what has been reported by Ahmed et al. (2012) who found that maternal hypothyroidism in rats reduced the proliferation, migration, and differentiation of the cerebellar granule cells, besides decreasing myelination of the neuronal axons and the dendrites of Purkinje cells of the offspring. Also, perinatal iodine deficiency and hypothyroidism in rats were reported to delay granular cell migration, increase apoptosis of IGL and impair late differentiation pattern of Golgi cells and the genesis of Purkinje cell dendrites (Wang et al., 2012).

Functionally, the Purkinje cells represent the sole modulatory output from the cerebellar cortex into the deep cerebellar nuclei. At the level of these deep nuclei, excitatory input collaterals from the mossy and climbing fibers converge with the inhibitory inputs from the Purkinje cells. Finally, the deep nuclei send diverse cerebellar outputs (nucleofugal fibers) to the cerebral

cortex, subcortical regions, brain stem, and spinal cord that constitute the main cerebellar functional connections. Via these connections the cerebellum is substantially involved in the coordination of voluntary movements, motor learning, cognitive functions, and maintenance of balance (Roostaei et al., 2014).

In this work, Purkinje cells revealed shrinkage and nuclear pyknosis in the three BDE-47 offspring subgroups. This detrimental effect of BDE-47 on the Purkinje cells could be the possible cause beyond the concomitant impairment of the functional domains of the cerebellum with motor incoordination in BDE-47 offspring. These offspring exhibited a significant decrease of the balancing time spent at the rotarod test. In line with this functional drawback of BDE-47, it was reported that perinatal exposure to low doses of BDE-47 disturbed spontaneous locomotor activity in the rat pups (Suvorov et al., 2009). Also, it was found that a postnatal exposure of mice to BDE-47 led to behavioral abnormalities, particularly those related to motor function and cognition (Gee and Moser, 2008). Additionally, a perinatal exposure of dams to BDE-47 leads to decreased locomotion in the open field, and a slower swim speed in the Morris water maze in mice pups (Ta et al., 2011).

The proposed mechanism of BDE-47 induced motor incoordination and disturbed locomotor activity could be secondary to its effect on the frontal lobe that in turn affects the cerebellum due to the extensive connection between these two brain structures, particularly in executing the motor functions. This mechanism was adopted by Byun et al. (2015) who found a decreased DNA methylation pattern of the brain mitochondrial cytochrome c oxidase encoded gene secondary to increased reactive oxygen species in the frontal lobe of the rat offspring perinatally exposed to BDE-47. The defects in cytochrome c oxidase structure are known to cause various metabolic and functional disorders of the brain.

Additionally, one of the potential toxic effects of BDE-47 is via the epigenetic mechanisms which are major driving forces of dysregulation of gene transcription that hamper the normal neurodevelopment processes with subsequent functional disability. In that issue, exposure to 6-OH-BDE-47 (a BDE-47 metabolite) was reported to interfere with the neurodevelopmental chromatin remodeling mechanisms and gene transcription programs, which in turn interfere with downstream processes such as synapse development and overall functional maturity of neurons (Poston et al., 2018).

Moreover, BDE-47 induced motor incoordination may be attributed to the disruption of thyroid hormone homeostasis that are essential for normal cerebellar development and functions (Ahmed et al., 2012). In this context, gestational hypothyroidism was reported to be associated with a large number of morphological and behavioral defects on the developing brain of animals and humans (Zoeller and Crofton, 2005).

Biologically, normal neuronal development requires the presence of one or more of the neurotrophins like NGF, BDNF, neurotrophin-3 (NT-3), neurotrophin-4 (NT-4/5), and NT-6 which are regulatory factors that mediate the differentiation and survival of neurons via activating specific neuronal signaling pathways (Poo, 2001; Gilbert and Lasley, 2013). In that regard, in the current study, to elaborate the growth modulating role of the neurotrophins in the postnatal development of the cerebellar cortex, we have evaluated the immunoreaction and optical density of two crosstalk- relating neurotrophins NGF, and BDNF in the cytoplasm of cerebellar neurons. Upon immunohistochemical study, we have found that, in comparison to the control offspring, the three BDE-47 offspring subgroups displayed lesser NGF and BDNF immunoreactions in the cytoplasm of the granule cells in the EGL and the IGL and in the neuropil of ML, together with decreased mean optical density of NGF and BDNF in the immuno-stained cerebellar sections. This reduced immuno expression of NGF and BDNF can be attributed to the BDE-47 induced decline of the serum thyroid hormones levels that was evident in this study. In line with our explanation, Sinha et al. (2009) found that perinatal hypothyroidism impaired the expression of NGF and BDNF. In addition, BDE-47 and 6-OH-BDE-47 were reported to have neurotoxic potentials by disturbing calcium homeostasis and triggering mitochondrial dysfunction and oxidative stress that may indirectly perturb the neurotrophins (Dingemans et al., 2008).

Not only a decline in NGF and BDNF immune-expression, but also the proliferating cell nuclear antigen (PCNA) was down regulated in the cerebellar cortical sections of the three BDE-47 offspring subgroups. This detrimental effect may be related to the oxidative stress and apoptotic neuronal cell death induced by BDE-47 with a consequent developmental neurotoxicity as was documented in the invitro and in vivo study conducted in mice (Costa et al., 2015). As a matter of fact, the developing brain is highly sensitive to oxidative stress, possibly due to its high levels of unsaturated lipids and limited antioxidant capacity (Sola et al., 2007). In line with this vulnerability of the developing brain cells, He et al. (2008) and Zhang et al. (2016) have reported that secondary to oxidative stress, BDE-47 disturbed the calcium-dependent signaling transduction and caused apoptosis and DNA damage. The later sequelae alter the neurodevelopmental processes through alterations of the gene transcription (Wells et al., 2010). In addition, BDE-47 uncouples the mitochondria electron transport chain and inhibits energy production necessary for vital functions of the brain cells (Pazin et al., 2015). Interestingly, in this study, BDE-47 offspring exhibited congested blood capillaries and focal areas of hemorrhage in the white matter core of some cerebellar lobules, particularly on PND21, that implies an inflammatory effect of BDE-47 (Park and Loch-Caruso, 2014). Also, multiple Bergmann glia (BG) cells under light microscopic examination with a strong PCNA

immunoreaction of these cells on the PND14 and PND21 were observed compared with those found in age-matched control offspring. Actually, BG cells are astrocytes derived from the radial glia cells and found in the PCL nearby the Purkinje cells and they have a unique anti-inflammatory role via secreting anti-inflammatory cytokines and provide a scaffold for granule cell migration (Yamada and Watanabe, 2002).

In this work, in order to clarify the extent of synaptogenesis inside the cerebellar cortex, we assessed the synaptic density in the cerebellar sections indirectly through IHC staining of synaptophysin (SYN) (Yao et al., 2002). Specifically, the ML is characterized by the presence of a remarkable synaptic density between various neurons including the parallel fibers of the granule cells, the flattened dendritic trees of Purkinje cells and the inhibitory interneurons (stellate and basket cells) in ML. Also, the GCL is characterized by the presence of interlacing synaptic structures called "cerebellar glomeruli" that are formed of synaptic connections between the mossy fiber terminals with many dendrites of the granule cells and the dendrites of Golgi cells (Roostaei et al., 2014).

In comparison to the corresponding age matched control, the histological results of the three BDE-47offspring subgroups revealed thinner ML and lesser cerebellar glomeruli in the GCL. In addition, IHC results displayed weak SYN immunoreaction at the surface of Purkinje cells, in the neuropil of ML and in cerebellar glomeruli of GCL together with decreased mean optical SYN density. These findings implied indirectly a decreased in the synaptic density within the cerebellar cortical layers that reflected a delay in the postnatal development of the cerebellar cortex and for sure implied an impairment of the cerebellar functions.

The decrease in the synaptic density in BDE-47 offspring can be attributed to the concomitant decrease of the mean optical density of BDNF that was encountered in this study. The BDNF signaling pathways were reported to promote the synaptic transmission via modulating the synaptic vesicle-associated proteins (synapsin, synaptophysin and synaptobrevin) (Jovanovic et al., 2000). Also, the decreased synaptic density can be explained on the basis of the toxic effect of most PBDEs congeners that have been shown to interfere with signal transduction pathways, such as protein kinase C (Madia et al., 2004), and perturbation of calcium homeostasis in several neuronal precursors (Gassmann et al., 2014). Moreover, Ibhazehiebo et al. (2011) have observed that perinatal hypothyroidism caused by PBDEs was associated with decreased dendrite arborization and synaptogenesis of the Purkinje cells.

Finally, it was reported that NGF played a great role in the normal proliferation of the immature granule neurons and the differentiation of Purkinje cells of the cerebellum (Legrand and Clos, 1991). NGF has surface receptors on the axon terminals and upon binding to these receptors it is internalized and transported in a retrograde manner to the soma of the neurons, where it is involved in the neuronal survival and synaptic transmission at the dendrites (Poo, 2001). The later function of NGF might explain why in the control offspring there was an intense immune-expression of NGF in the neuropil of the ML that has numerous synaptic connections, although BDE-47 offspring exhibited a decrease in NGF expression that perturbed the synaptic density between the cerebellar neurons in the ML.

Conclusion

In the light of our results, we concluded that maternal exposure to BDE-47 during pregnancy and lactation has a retarding influence on the postnatal development of the rat cerebellar cortex. These detrimental effects of BDE-47 might be due to its down regulating effects on the thyroid hormones, NGF, BDNF and impaired proliferation and synaptogenesis.

References

Ahmed O.M., Ahmed R.G., El Gareib A.W., El Bakry A.M. and Abd El Tawab S.M. (2012). Effects of experimentally induced maternal hypothyroidism and hyperthyroidism on the development of rat offspring: II-the developmental pattern of neurons in relation to oxidative stress and antioxidant defense system. Int. J. Devel. Neurosci. 30, 517-537.

Bansal R., Tighe D., Danai A., Rawn D.F., Gaertner D.W., Arnold D.L. and Zoeller R.T. (2014). Polybrominated diphenyl ether (DE-71) interferes with thyroid hormone action independent of effects on circulating levels of thyroid hormone in male rats. Endocrinology. 155, 4104-4112.

Byun H., Benachour N., Zalko D., Frisardi M.C., Colicino E., Takser L. and Baccarelli A.A. (2015). Epigenetic effects of low perinatal doses of flame retardant BDE-47 on mitochondrial and nuclear genes in rat offspring. Toxicology 328, 152-159.

Costa L.G. and Giordano G. (2007). Developmental neurotoxicity of polybrominated diphenyl ether (PBDE) flame retardants. Neurotoxicology 28, 1047-1067.

Costa L.G., Pellacani C., DaoK, Kavanagh T.J. and Roque P.J. (2015). The brominated flame retardant BDE47 causes oxidative stress and apoptotic cell death in vitro and in vivo in mice. Neurotoxicology 48, 68-76.

Dingemans M.M., Groot A., De Kleef R.G.V., Bergman A°., Berg M.V.D., Vijverberg H.P. and Westerink R.H. (2008). Hydroxylation increases the neurotoxic potential of BDE-47 to affect exocytosis and calcium homeostasis in PC12 cells. Environ. Health Perspect. 116, 637-643.

Djatchkova-Podkletnova I. and Alho H. (2005). Alterations in the development of rat cerebellum and impaired behavior of juvenile rats

after neonatal 6-OHDA treatment. Neurochem. Res. 30, 1599-1605.

Dorman D.C., Chiu W., Hales B.F., Hauser R., Johnson K.J., Mantus E., Martel S., Robinson K.A., Rooney A.A., Rudel R., Sathyanarayana S., Schantz S.L. and Waters K.M. (2018). Polybrominated diphenyl ether (PBDE) neurotoxicity: a systematic review and meta-analysis of animal evidence. J. Toxicol. Environ. Health B Crit. Rev. 21, 269-289.

Fonnum F. and Lock E.A. (2000). Cerebellum as a target for toxic substances. Toxicol. Lett. 112-113, 9-16.

Galas L., Bénard M., Lebon A., Komuro Y., Schapman D., Vaudry H., Vaudry D. and Komuro H. (2017). Postnatal migration of cerebellar interneurons. Brain Sci. 7, 62.

Gassmann K., Schreiber T., Dingemans M., Krause G., Roderigo C, Giersiefer S., Schuwald J., Moors M., Unfried K. and Bergman A. (2014). BDE-47 and 6-OH-BDE-47 modulate calcium homeostasis in primary fetal human neural progenitor cells via ryanodine receptor-independent mechanisms. Arch. Toxicol. 88, 1537-1548.

Gee J.R. and Moser V.C. (2008). Acute postnatal exposure to brominated diphenylether 47 delays neuromotor ontogeny and alters motor activity in mice. Neurotoxicol. Teratol. 30, 79-87.

Gilbert M.E. and Lasley S.M. (2013). Developmental thyroid hormone insufficiency and brain development: a role for brain-derived neurotrophic factor (BDNF)? Neuroscience 239, 253-270.

González-Maciel A., Romero-Velázquez R.M., Alfaro-Rodríguez A., Aparicio P.S. and Reynoso-Robles R. (2020). Prenatal exposure to oxcarbazepine increases hippocampal apoptosis in rat offspring. J. Chem. Neuroanat. 103, 101729.

He P., He W., Wang A., Xia T., Xu B. and Chen X. (2008). PBDE-47 induced oxidative stress, DNA damage and apoptosis in primary cultured rat hippocampal neurons. Neurotoxicology 29, 124-129.

Hites R.A. (2004). Polybrominated diphenyl ethers in the environment and in people: a meta-analysis of concentrations. Environ. Sci. Technol. 38, 945-956.

Hooper K. and McDonald T.A. (2000). The PBDEs: an emerging environmental challenge and another reason for breast-milk monitoring programs. Environ. Health Perspect. 108, 387-392.

Huang S.C., Giordano G. and Costa L.G. (2010). Comparative cytotoxicity and intracellular accumulation of five polybrominated diphenyl ether congeners in mouse cerebellar granule neurons. Toxicol. Sci. 114, 124-132.

Huang S., Cui Y., Guo X., Wang L., Li S., Lu Y., Bi Y., Huang X., Lin M., Xia Y., Wang S., Wang X., Zhou Z. and Sha J. (2015). 2,2',4,4'-Tetrabromodiphenyl ether disrupts spermatogenesis, impairs mitochondrial function and induces apoptosis of early leptotene spermatocytes in rats. Reprod. Toxicol. 51, 114-124.

Ibhazehiebo K., Iwasaki T., kurod J.k., Miyazaki W., Shimokawa N. and Koibuchi N. (2011). Disruption of thyroid hormone receptor - mediated transcription and thyroid hormone-induced Purknje cell dendrite arborization by poly brominated diphenyl ethers. Environ. Health Perspect. 119, 168-175.

Jovanovic J.N., Czernik A.J., Fienberg A.A., Greengard P. and Sihra T.S. (2000). Synapsins as mediators of BDNF-enhanced neurotransmitter release. Nat. Neurosci. 3, 323-329.

Khalil A., Parker M., Brown S.E., Cevikae S.E., Guo L.W., Jensen J., Olmsteda A., Portmana D., Wua H. and Suvorov A. (2017). Perinatal exposure to 2,2',4'4'-Tetrabromodiphenyl ether induces testicular toxicity in adult rats. Toxicology 389, 21-30.

Kodavanti P.R.S., Royland J.E., Osorio C., Winnik W.M., Ortiz P., Lei L. and Alzate O. (2015). Developmental exposure to a commercial PBDE mixture: effects on protein networks in the cerebellum and hippocampus of rats. Environ. Health Perspect. 123, 428-436.

Koenig C.M., Lango J., Pessah I.N. and Berman R.F. (2012). Maternal transfer of BDE-47 to offspring and neurobehavioral development in C57BL/6J mice. Neurotoxicol. Teratol. 34, 571-580.

Koning I.V., Tielemans M.J., Hoebeek F.E., Ecury-Goossen G.M., Reiss I.K., Steegers-Theunissen R.P. and Dudink J. (2017). Impacts on prenatal development of the human cerebellum: a systematic review. J. Matern. Fetal Neonatal. Med. 30, 2461-2468.

Lam J., Lanphear B.P., Bellinger D., Axelrad, D.A., McPartland J., Sutton P., Davidson L., Daniels N., Sen S. and Woodruff T.J. (2017). Developmental PBDE exposure and IQ/ ADHD in childhood: a systematic review and meta-analysis. Environ. Health Perspect.125, 086001.

Larsell O. and Jansen J. (1972). The comparative anatomy and histology of the cerebellum. The human cerebellum, cerebellar connections, and cerebellar cortex. University of Minnesota Press. Minneapolis.

Legrand C. and Clos J. (1991). Biochemical, immunocytochemical and morpho- logical evidence for an interaction between thyroid hormone and nerve growth factor in the developing cerebellum of normal and hypothyroid rats. Dev. Neurosci. 13, 382-396.

Madia F., Giordano G., Fattori V., Vitalone A., Branchi I. and Capone F. (2004). Differential in vitro neurotoxicity of the flame retardant PBDE-99 and of the PCB Aroclor 1254 in human astrocytoma cells. Toxicol. Lett. 154, 11-21.

Nagayach A., Patro N. and Patro I. (2014). Experimentally induced diabetes causes glial activation, glutamate toxicity and cellular damage leading to changes in motor function. Front. Cell. Neurosci. 8, 355.

Ni H.G., Ding, C., Lu, S.Y., Yin, X.L. and Samuel S.O. (2012). Food as a main route of adult exposure to PBDEs in Shenzhen, China. Sci. Total Environ. 437, 10-14.

Park H.R. and Loch-Caruso R. (2014). Protective effect of nuclear factor E2-related factor 2 on inflammatory cytokine response to brominated diphenyl ether-47 in the HTR-8/SVneo human first trimester extravillous trophoblast cell line. Toxicol. Appl. Pharmacol. 281, 67-77.

Pazin M., Pereira L.C. and Dorta D.J. (2015). Toxicity of brominated flame retardants, BDE-47 and BDE-99 stems from impaired mitochondrial bioenergetics. Toxicol. Mech. Methods 25, 34-41.

Poo M.M. (2001). Neurotrophins as synaptic modulators. Nat. Rev. Neurosci. 2, 24-32.

Poston R.G., Dunn C.J., Sarkar P. and Saha R.N. (2018). Persistent 6-OH-BDE-47 exposure impairs functional neuronal maturation and alters expression of neurodevelopmentally-relevant chromatin remodelers. Environ. Epigenet. 4, 20.

Rahimi-Balaei M., Bergen H., Kong J. and Marzban H. (2018). Neuronal migration during development of the cerebellum. Front. Cell. Neurosci. 12, 484.

Ramos-Vara J.A. and Miller M.A. (2014). When tissue antigens and antibodies get along: Revisiting the technical aspects of immunohistochemistry - The red, brown, and blue technique. Vet. Pathol. 51, 42-87.

Rees S., Harding R. and Walker D. (2008). An adverse intrauterine environment: implications for injury and altered development of the brain. Int. J. Dev. Neurosci. 26, 3-11.

Roostaei T., Nazeri A., Sahraian M.A. and Minagar A. (2014). The human cerebellum: a review of physiologic neuroanatomy. Neurol. Clin. 32, 859-869.

Sałat K., Librowski T., Nawiesniak B. and Gluch-Lutwin M. (2013). Evaluation of analgesic, antioxidant, cytotoxic and metabolic effects of pregabalin for the use in neuropathic pain. Neurol. Res. 35, 948-958.

Sánchez-Villagra M.R. and Sultan F. (2002). The cerebellum at birth in therian mammals, with special reference to rodents. Brain Behav. Evol. 59, 101-113.

Shevelkin A.V., Ihenatu C. and Pletnikov M.V. (2014). Pre-clinical models of neurodevelopmental disorders: focus on the cerebellum. Rev. Neurosci. 25, 177-194.

Sinha R.A., Pathak A., Kumar A., Tiwari M., Shrivastava A. and Godbole M.M. (2009). Enhanced neuronal loss under perinatal hypothyroidism involves impaired neurotrophic signaling and increased proteolysis of p75(NTR). Mol. Cell. Neurosci. 40, 354-364.

Sola A., Rogido M.R. and Deulofeut R. (2007). Oxygen as a neonatal health hazard: call for detente in clinical practice. Acta Paediatr. 96, 801-812.

Suvarna K.S., Layton C. and Bancroft J.D. (2018). Bancroft's theory and practice of histological techniques E-Book. Elsevier Health Sciences.

Suvorov A., Battista M.C. and Takser L. (2009). Perinatal exposure to low-dose 2,20,4,40-tetrabromodiphenyl ether affects growth in rat offspring: what is the role of IGF-1?. Toxicology 260, 126-131.

Suvorov A. and Takser L. (2010). Global gene expression analysis in the livers of rat offspring perinatally exposed to low doses of 2,2',4,4'-tetrabromodiphenyl ether. Environ. Health Perspect. 118, 97-102.

Ta T.A., Koenig C.M., Golub M.S., Pessah I.N., Qi L. and Aronov P.A. (2011). Bioaccumulation and behavioral effects of 2,2',4,4'-tetrabromodiphenyl ether (BDE-47) in perinatally exposed mice. Neurotoxicol. Teratol. 33, 393-404.

Talsness C.E., Kuriyama S.N., Sterner-Kock A., Schnitker P., Grande S.W., Shakibaei M., Andrade A., Grote K. an d Chahoud I. (2008). In utero and lactational exposures to low doses of polybrominated diphenyl ether-47 alter the reproductive system and thyroid gland of female rat offspring. Environ. Health Perspect. 116, 308-314.

Vuong A.M., Yolton K., Dietrich K.N., Braun J.M., Lanphear B.P. and Chen A. (2018). Exposure to polybrominated diphenyl ethers (PBDEs) and child behavior: Current findings and future directions. Horm. Behav. 101, 94-104.

Wang Y., Zhong J., Xu H., Wei W., Dong J., Yu F., Wang Y., Gong J., Shan Z., Teng W. and Chen J. (2012). Perinatal iodine deficiency and hypothyroidism increase cell apoptosis and alter double cortin and reelin protein expressions in rat cerebellum. Arch. Med. Res. 43, 255-264.

Wells P.G., McCallum G.P., Lam K.C. Henderson J.T. and Ondovcik S.L. (2010). Oxidative DNA damage and repair in teratogenesis and neurodevelopmental deficits. Birth Defects Res. C Embryo Today 90,103-109.

Wu H., Cao L., Li F., Lian P. and Zhao J. (2015). Multiple biomarkers of the cytotoxicity induced by BDE-47 in human embryonic kidney cells. Chemosphere 126, 32-39.

Yamada K. and Watanabe M. (2002). Cytodifferentiation of Bergmann glia and its relationship with purkinje cells. Anat. Sci. Int. 77, 94-108.

Yao I., Iida J., Nishimura W. and Hata Y. (2002). Synaptic and nuclear localization of brain enriched guanylate kinase-associated protein. J. Neurosci. 22, 5354-5364.

Zhang S., Chen Y., Wu X., Gao H., Ma R., Jiang C., Kuang G., Zhao G., Xia T., Zhang X., Lei R., Zhang C., Li P., Xu C. and Wang A. (2016). The pivotal role of Ca(2+) homeostasis in PBDE-47-induced neuronal apoptosis. Mol. Neurobiol. 53, 7078-7088.

Zoeller R.T. and Crofton K.M. (2005). Mode of action: developmental thyroid hormone insufficiency: neurological abnormalities resulting from exposure to propylthiouracil. Crit. Rev. Toxicol. 35, 771-781.